Inorg. Chem. **2002**, *41*, 2785–2794

Coordination Chemistry and Reactivity of Monomeric Alkoxides and Amides of Magnesium and Zinc Supported by the Diiminato Ligand $CH(CMeNC_6H_3\text{-}2,6\text{-}^iPr_2)_2$. A Comparative Study

Malcolm H. Chisholm,* Judith Gallucci, and Khamphee Phomphrai

Department of Chemistry, Newman & Wolfrom Laboratories, The Ohio State University, 100 W. 18th Avenue, Columbus, Ohio 43210-1185

Received February 25, 2002

The preparation and characterization of a series of closely related magnesium and zinc compounds are reported: $LMg(N^iPr_2)(THF)$, **1**; $LZn(N^iPr_2)$, **2**; $LMg(O^tBu)(THF)$, **3**; $LZn(O^tBu)$, **4**; and $LZn(OSiPh_3)(THF)$, **6**; where L = $CH(CMeNC_6H_3\text{-}2,6\text{-}^iPr_2)_2$. Their dynamic solution behavior has been examined by variable-temperature NMR studies and reveals that THF reversibly dissociates in toluene-d_8 or CD_2Cl_2 and that exchange with free THF occurs by a dissociative process. Compounds **1**–**4** and **6** all initiate and subsequently sustain ring-opening polymerization (ROP) of lactides. For a related series of compounds $LMX(THF)_n$, where $n = 1$ or 0, the rate of initial ring-opening follows the order M = Mg > Zn and X = $O^tBu > N^iPr_2 > NSi_2Me_6 > OSiPh_3$. In THF at 25 °C, compounds **3** and **4** polymerize 100 equiv of *rac*-lactide to >95% conversion in 5 and 80 min for M = Mg and Zn, respectively, and yield ca. 90% heterotactic PLA, (*isi* + *sis* tetrads). The reactions proceed faster in methylene chloride, but for M = Mg, a Bernoulian distribution of tetrads is formed from *rac*-lactide (3*iii*:2*isi*:*sii*:*sis*:*iis*) prior to *trans*-esterification. Polymerization of L-LA in toluene-d_8 and THF-d_8 by **3** and **4** have been studied by VT ^{1}H NMR spectroscopy: the resting state for zinc is proposed to be a monomeric species akin to $LZn(\eta^2\text{-}OCHMeC(O)OMe)$, whereas the magnesium complex appears to be dimeric $LMg(\mu\text{-}OP)_2MgL$. None of the compounds is capable of initiating homopolymerization of propylene oxide (PO) or cyclohexene oxide (CHO), although the magnesium amide **1** effects ring-opening by allylic proton abstraction and the dimeric compound $[LMg(\mu\text{-}OC_6H_9)]_2$, **7**, is formed. Reactions with carbon dioxide are also described, along with the characterization of $LZnO_2CN^iPr_2$, **8**, which is shown to be inert with respect to CHO and PO at room temperature. All the compounds are hydrolytically sensitive, and $LZn(\mu\text{-}OH)_2ZnL$, **5**, has been isolated from hydrolysis of compound **4**. The crystal and molecular structures are reported for compounds **1**–**5**, **7**, and **8**. These results are compared with those recently reported by Coates et al. (*J. Am. Chem. Soc.* **2001**, *123*, 3229–3238).

Introduction

The elements magnesium and zinc share many similar properties. They form M^{2+} salts and have very similar ionic radii.[1] They are both essential for life, yet nature employs them in very different ways.[2] Magnesium (2+) can be considered a hard metal, while zinc (2+) is soft.[3] However, just how this translates into chemical reactivity is not always predictable. Indeed, there are relatively few examples of closely related reactions involving both metals wherein the coordination sphere is identical.[4] In this paper, we set out to describe the chemistry of closely related compounds of magnesium and zinc supported by the β-diiminato ligand $CH(CMeNC_6H_3\text{-}2,6\text{-}^iPr_2)_2$ = L. These compounds have the formula $LMX(THF)_n$, where X = N^iPr_2, O^tBu and $n = 1$ or 0. We examine these monomeric compounds in terms of their solid-state molecular structures, their dynamic solution behavior, and their reactivity toward lactides, epoxides, and carbon dioxide. These studies complement the recent elegant

(1) Cotton, F. A.; Wilkinson, E.; Murillo, C. A.; Bochmann, M. *Advanced Inorganic Chemistry*, 6th ed.; John Wiley & Sons: New York, 1999; pp 1302−1304.

(2) Campbell, N. A. *Biology*, 3rd ed.; Benjamin/Cummings Publishing Co.: California, 1993; pp 718−722, 811−814.

(3) Huheey, J. E.; Keiter, E. A.; Keiter, R. L. *Inorganic Chemistry: Principles of Structure and Reactivity*, 4th ed.; Harper Collins College Publishers: New York, 1993; pp 344−348.

(4) Chisholm, M. H.; Eilerts, N. W.; Huffman, J. C.; Iyer, S. S.; Pacold, M.; Phomphrai, K. *J. Am. Chem. Soc.* **2000**, *122*, 11845−11854.

10.1021/ic020148e CCC: $22.00
Published on Web 04/25/2002

work described by Coates' group, who have studied a family of β-diiminato zinc isopropoxide complexes, $[L'Zn(\mu\text{-}O^iPr)]_2$, and shown these to be active in the ring-opening polymerization (ROP) of lactides[5] and the copolymerization of cyclohexene oxide (CHO) and carbon dioxide.[6] Brief mention has also been made by both Coates and us[7] of related magnesium alkoxides in the ROP of lactides.

Results and Discussion

Syntheses. The synthesis of related magnesium and zinc compounds by metathetic reactions would, at first, seem a rather trivial affair. However, we have found this not to be the case. Indeed, the reason for this could not always be explained, and even when determined, it proved puzzling.

LMg(N^{i}Pr$_2$)(THF), 1. The reaction between $Mg(N^iPr_2)_2$ and the free β-diiminato ligand LH (1 equiv) in refluxing THF proved successful in the preparation of compound **1**. In this reaction, proton transfer occurs with the elimination of HN^iPr_2. This reaction does not occur in toluene or benzene under reflux. The compound is very air- and moisture-sensitive and forms light green crystals from cooled concentrated THF solutions.

LZn(N^{i}Pr$_2$), 2. Our best preparative route to this compound involved the direct reaction between LiN^iPr_2 (2 equiv) and LH in THF, stirred for 30 min at room temperature, followed by the addition of a solution of $ZnCl_2$ in THF. Subsequent extraction of the dried residue with hexane gave compound **2**, which gives light green crystals upon recrystallization from hexane. This compound is also air- and moisture sensitive.

LMg(OtBu)(THF), 3, can be prepared by the addition of ^{t}BuOH (1 equiv) to a hydrocarbon solution of **1** and may be prepared in a one-pot procedure without the isolation of **1**, as described in the Experimental Section. Compound **3** is a white hydrocarbon-soluble air-sensitive material.

LZn(O^{t}Bu), 4. The preparation of this compound proved very problematic. Addition of ^{t}BuOH to $LZnNSi_2Me_6$ does not lead to any reaction under the conditions that Coates[8] used to prepare the related isoproxide $[LZn(\mu\text{-}O^iPr)]_2$ by the addition of ^{i}PrOH. The more reactive $LZn(N^iPr_2)$, compound **2**, readily reacts with ^{t}BuOH in solvents such as hexane, toluene, and THF at room temperature, but no simple product is obtained in these reactions. However, by combining two toluene solutions cooled to -78 °C, one of compound **2** and the other containing ^{t}BuOH (1 equiv), compound **4** is formed in near quantitative yield. This compound can be recrystallized from toluene. It is air- and moisture-sensitive and is labile to formation of a μ-hydroxide, $LZn(\mu\text{-}OH)_2ZnL$, **5**.

LZn(OSiPh$_3$)(THF), 6, is readily prepared by the addition of Ph_3SiOH (1 equiv) to either $LZnNSi_2Me_6$ or $LZn(N^iPr_2)$ in THF solvent. This compound is a white, air-sensitive, crystalline compound soluble in common hydrocarbon solvents.

[LMg(μ-OC$_6$H$_9$)]$_2$, 7. A benzene solution of **1** or $LMgNSi_2Me_6$ reacts with cyclohexene oxide to form compound **7** as a colorless crystalline solid that is very sparingly soluble in benzene or toluene. Compound **7** is formed by allylic proton abstraction by the amide bound to magnesium.

LZn(O$_2$CN^{i}Pr$_2$), 8. The addition of CO_2 to compound **2** in benzene at room temperature leads to the formation of compound **8** in quantitative yield. Compound **8** is readily soluble in hydrocarbon solvents and may be recrystallized from toluene as a white, air-sensitive material.

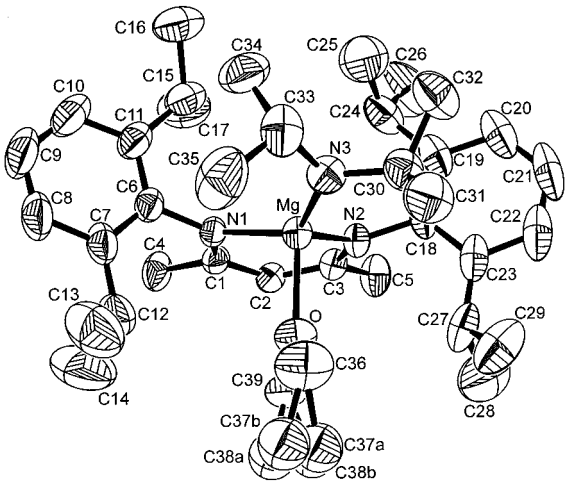

Figure 1. ORTEP drawing of $LMg(N^iPr_2)(THF)$ showing the pseudotetrahedral geometry at the Mg center. Thermal ellipsoids are drawn at the 50% probability level. Hydrogen atoms are omitted for clarity. The disorder of the methylene carbon atoms is shown by the presence of C37, C38 in both a and b sites.

Table 1. Selected Bond Distances (Å) and Angles (deg) for $LMg(N^iPr_2)(THF)$

A	B	distance	A	B	C	angle
Mg	N1	2.091(2)	N1	Mg	N2	92.79(7)
Mg	N2	2.071(2)	N1	Mg	N3	131.28(9)
Mg	N3	1.968(2)	N1	Mg	O	99.27(8)
Mg	O	2.092(2)	N2	Mg	N3	120.04(9)
			N2	Mg	O	99.37(8)
			N3	Mg	O	108.49(8)

Single Crystal and Molecular Structures. LMg(N^{i}Pr$_2$)(THF), 1. An ORTEP drawing of the molecular structure of **1** is given in Figure 1. The view of the molecule shows the disorder of the THF ligand and shows how this ligand fits within a pocket created by two of the isopropyl groups of the β-diiminate ligand. The diisopropylamide ligand has its NC_2 plane perpendicular to the Mg−O(THF) axis and is nearly contained in the N(1)−Mg−N(2) plane of the β-diiminate.

Selected bond distances and angles are given in Table 1. The Mg−N^{i}Pr$_2$ bond distance, 1.97 Å, is 0.1 Å shorter than the Mg−N distances to the β-diiminate, 2.08 Å (ave), which are comparable to the Mg−O(THF) distance, 2.09 Å. The N−Mg−N angle associated with L is 92°, while the other N−Mg−N angles are 131° and 120°. The sum of the N−Mg−N angles is 344°, which is between that expected

(5) Chamberlain, B. M.; Cheng, M.; Moore, D. R.; Ovitt, T. M.; Lobkovsky, E. B.; Coates, G. W. *J. Am. Chem. Soc.* **2001**, *123*, 3229−3238.
(6) Cheng, M.; Moore, D. R.; Reczek, J. J.; Chamberlain, B. M.; Lovkovsky, E. B.; Coates, G. W. *J. Am. Chem. Soc.* **2001**, *123*, 8738−8749.
(7) Chisholm, M. H.; Huffman, J. C.; Phomphrai, K. *J. Chem. Soc., Dalton Trans.* **2001**, 222−224.
(8) Cheng, M.; Attygalle, A. B.; Lobkovsky, E. B.; Coates, G. W. *J. Am. Chem. Soc.* **1999**, *121*, 11583−11584.

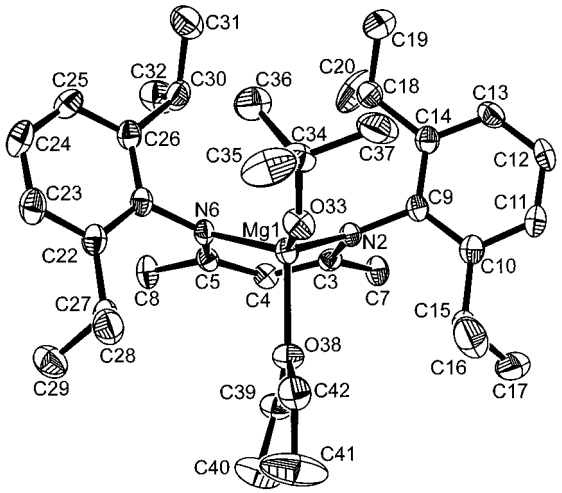

Figure 2. ORTEP drawing of LMg(O^{t}Bu)(THF) with thermal ellipsoids drawn at the 50% probability level. Hydrogen atoms are omitted for clarity.

Table 2. Selected Bond Distances (Å) and Angles (deg) for LMg(O^{t}Bu)(THF)

A	B	distance	A	B	C	angle
Mg1	O33	1.844(2)	O33	Mg1	O38	98.77(9)
Mg1	O38	2.048(2)	O33	Mg1	N2	127.8(1)
Mg1	N2	2.054(2)	O33	Mg1	N6	126.1(1)
Mg1	N6	2.059(2)	O38	Mg1	N2	103.79(9)
C2	C3	1.325(5)	O38	Mg1	N6	105.15(9)
			N2	Mg	N6	92.20(9)

for a tetrahedral MgN_3O moiety (328.5°) and a trigonal N_3-Mg unit (360°). The O−Mg−N angles span the range of 99°−108°, with the latter including the N^{i}Pr$_2$ nitrogen. The orientation of the 2,6-^{i}Pr$_2$C$_6$H$_3$ groups in this structure is as seen in the others reported in this work and as previously seen in the compounds $LMNSi_2Me_6$, where M = Mg and Zn, reported by Coates.[6]

LMg(O^{t}Bu)(THF), 3. An ORTEP drawing of compound **3** is given in Figure 2, and selected bond distances and bond angles are given in Table 2. The view shown in Figure 2 emphasizes the similarity to the structure just described for LMg(N^{i}Pr$_2$)(THF), **1**. The Mg−O distances are 1.84 and 2.05 Å to the tertiary butoxide and THF ligands, respectively. The Mg−O(THF) distance is shorter in this compound than that seen in the amide, compound **1**. The Mg−N distances associated with the β-diiminate ligand are also very slightly shorter, 2.06 Å (ave) in **3** versus 2.08 Å (ave) in **1**. The sum of the N−Mg−N and N−Mg−O angles involving the O^{t}Bu ligand is 346°, once again implying a significant distortion from tetrahedral geometry. Indeed, the structures of **1** and **3** may be viewed as flattened tetrahedra formed by the uptake of a THF ligand by a trigonal LMX molecule. The THF ligand is oriented within the pocket formed by the 2,6-^{i}Pr$_2$C$_6$H$_3$ groups, as is the Mg−O−CMe$_3$ group, which has a Mg−O−C angle of 135°.

LZn(N^{i}Pr$_2$), 2. An ORTEP drawing of the three-coordinate zinc amide is given in Figure 3, and selected bond distances and angles are given in Table 3. This molecule contains a planar ZnN_3 moiety, and the NC_2 unit of the N^{i}Pr$_2$ ligand is disordered over two sites. The dihedral angle between the NC_2 plane of the N^{i}Pr$_2$ ligand and the ZnN_2 plane of the β-diiminate is 43.5°. The disorder leads to 50:50 left- and right-handed pitches of the NC_2 plane. Clearly, from purely steric considerations, we might have expected the NC_2 unit to be perpendicular to the ZnN_3 plane. We propose that the adoption of the propeller pitch of the NC_2 unit arises from a compromise of steric and electronic factors. If the NC_2 unit is contained in the ZnN_3 plane, maximum N p_π to Zn p_π bonding is possible, but the bulky C$_6$H$_3$-2,6-^{i}Pr$_2$ ligands impede this. The Zn−N distances are all roughly 0.1 Å shorter than their related distances in compound **1**. In part, this must be a reflection of the different coordination numbers, 4 for Mg in **1** and 3 for Zn in **2**. In the structurally related $LZnNSi_2Me_6$ compound prepared and characterized by Coates,[6] which also contains three coordinate zinc (2+) ions, the M−N distances differ by 0.044 Å to the amide nitrogen with the Zn−N^{i}Pr$_2$ having the shorter distance.

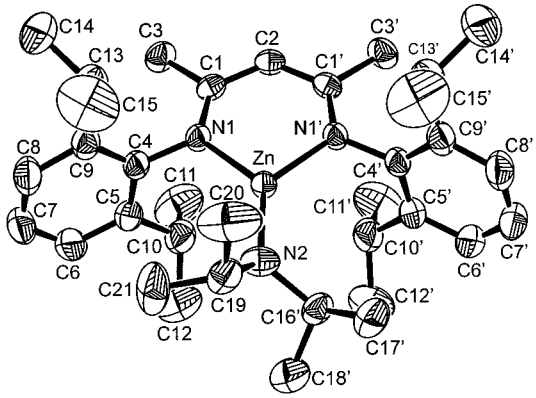

Figure 3. ORTEP drawing of LZn(N^{i}Pr$_2$) indicating the trigonal planar geometry at the Zn center. Thermal ellipsoids are drawn at the 50% probability level. Hydrogen atoms are omitted for clarity.

Table 3. Selected Bond Distances (Å) and Angles (deg) for LZnN^{i}Pr$_2$

A	B	distance	A	B	C	angle
Zn	N1	1.963(1)	N1	Zn	N1′	97.05(8)
Zn	N1′	1.963(1)	N1	Zn	N2	131.17(4)
Zn	N2	1.852(2)	N1′	Zn	N2	131.17(4)

LZn(O^{t}Bu), 4. An ORTEP drawing of this three-coordinate zinc(II) complex is given in Figure 4, and selected bond distances are given in Table 4. The Zn−N distances are notably shorter than in the amide compound **2**, and the Zn−O distance of 1.80 Å is 0.04 Å shorter than in LMg(O^{t}Bu)(THF). Again, in part, this can be attributed to the differing coordination numbers of the metal ions. The Zn−O−C angle is 138° and the orientation of the Zn−O−C plane allows O p_π to Zn p_π bonding. Note this orientation is quite different from that seen in the four-coordinate magnesium compound **2**.

LZn(μ-OH)$_2$ZnL, 5. The structure of this compound is reported in the Supporting Information. It is very similar to the molecular structure of L′Zn(μ-OH)$_2$ZnL′ recently reported by Coates,[6] where L′ = CH(CMeNC$_6$H$_3$-2,6-Et$_2$)$_2$.

[LMg(μ-OC$_6$H$_9$)]$_2$, 7. An ORTEP view of the dimeric alkoxide-bridged compound, **7**, is shown in Figure 5, and selected bond distances and angles are given in Table 5. The molecule has a crystallographically imposed center of inversion and a mirror plane containing the central Mg_2O_2 moiety. The oxygen atoms are not trigonal planar but are

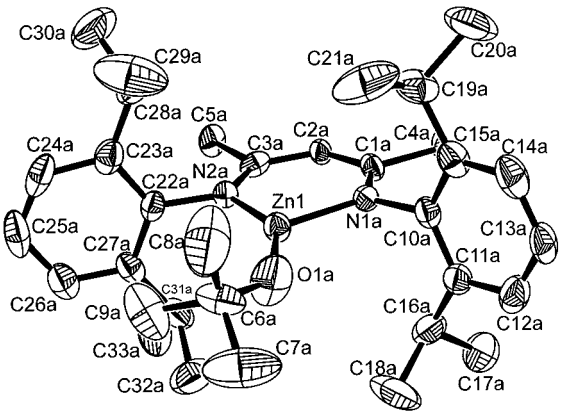

Figure 4. ORTEP drawing of LZn(O^{t}Bu) with thermal ellipsoids drawn at the 50% probability level. Hydrogen atoms are omitted for clarity.

Table 4. Selected Bond Distances (Å) and Angles (deg) for LZnO^{t}Bu

A	B	distance	A	B	C	angle
Zn1	O1a	1.800(5)	O1a	Zn1	N1a	117.8(2)
Zn1	N1a	1.931(5)	O1a	Zn1	N2a	142.8(2)
Zn1	N2a	1.917(5)	N1a	Zn1	N2a	99.1(3)

pyramidal, and the C_6 ring is disordered above and below the Mg_2O_2 plane. Within the C_6 ring, the C−C distances allow the identification of the C−C double bond, C(2)−C(3) = 1.325(5) Å, and clearly identify this ligand as a cyclohexenyl oxide formed by deprotonation of cyclohexene oxide at the allylic position. This compound is superficially related to the Coates[5,8] compounds $[LM(\mu\text{-}O^iPr)]_2$, and a direct comparison of M−N and M−O distances and angles is possible for the central $N_4M_2O_2$ skeletons. This is given is Table 6. These data reveal the structural similarities in these three molecules. Note that the Mg−O and Zn−O distances are virtually identical, though the Mg−N distances are significantly longer by 0.05 Å.

LZn(η^2-O$_2$CN^{i}Pr$_2$), 8. An ORTEP drawing of this monomeric four-coordinate zinc complex is given in Figure 6, and selected bond distances and angles are given in Table 7. An important but not unexpected observation is the planarity of the O_2CNC_2 unit of the carbamate ligand and the small O−Zn−O angle. It is also particularly interesting that this compound is monomeric when closely related zinc(II) complexes, $LZnO_2CMe$[9] and $LZnO_2CO^iPr$,[10] are dimeric in the solid-state having μ-η^1,η^1-O_2CX bridges.

Solution Behavior: NMR Studies. A trigonal planar molecule of formula LMX and a four-coordinate one of formula LMX_2 contain a molecular plane of symmetry, and by NMR spectroscopy, one observes two isopropyl methyl doublets as a result of restricted rotation about the aryl-carbon-to-nitrogen bond of the β-diiminato ligand. This situation is seen for the trigonal planar zinc compounds **2** and **4** and parallels the previous observation of Coates for compounds such as $LZnNSi_2Me_6$ and $[LZn(\mu\text{-Cl})]_2$.[6] However, for a four-coordinate compound of the type LM(X)(Y), such as in the THF adducts **1** and **3**, there are now four chemically inequivalent isopropyl methyl groups.

(9) Cheng, M.; Lobkovsky, E. B.; Coates, G. W. *J. Am. Chem. Soc.* **1998**, *120*, 11018−11019.
(10) Moore, D. R.; Coates, G. W. The 221st ACS National Meeting, San Diego, CA; Inorganic Division-232, April 2001.

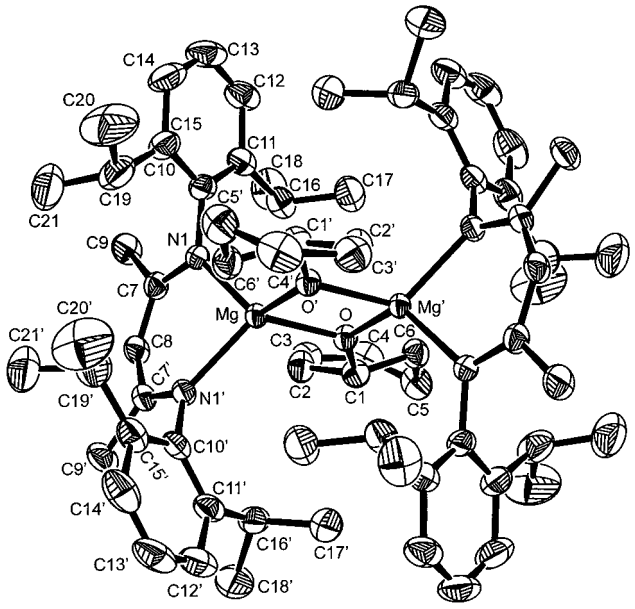

Figure 5. ORTEP drawing of $[LMg(\mu\text{-}OC_6H_9)]_2$ with thermal ellipsoids drawn at the 50% probability level. Hydrogen atoms are omitted for clarity.

Table 5. Selected Bond Distances (Å) and Angles (deg) for $[LMg(\mu\text{-}OC_6H_9)]_2$

A	B	distance	A	B	C	angle
Mg	O	1.970(2)	O	Mg	O′	81.44(6)
Mg	O′	1.994(2)	O	Mg	N1	125.10(4)
Mg	N1	2.110(1)	O	Mg	N1′	125.09(4)
			O′	Mg	N1	118.28(5)
			O′	Mg	N1′	118.28(5)
			N1	Mg	N1′	91.76(7)
			Mg	O	Mg′	98.56(6)

Table 6. Bond Distances (Å) and Angles (deg) around $N_4M_2O_2$ Skeletons of Dimeric $[LZn(\mu\text{-}O^iPr)]_2$, $[LMg(\mu\text{-}O^iPr)]_2$, and $[LMg(\mu\text{-}OC_6H_9)]_2$ in a Form of (N1)(N2)(M1)[μ-O1-μ-O2](M2)(N3)(N4)

	$[LZn(\mu\text{-}O^iPr)]_2$[a]	$[LMg(\mu\text{-}O^iPr)]_2$[a]	$[LMg(\mu\text{-}OC_6H_9)]_2$[b]
		Bonds	
M1−N1	2.074(4)	2.123(3)	2.110(1)
M1−N2	2.054(4)	2.114(3)	2.110(1)
M1−O1	1.983(3)	1.987(2)	1.994(2)
M1−O2	1.983(3)	1.978(2)	1.970(2)
		Angles	
N1−M1−N2	94.8(2)	91.3(1)	91.76(7)
N1−M1−O1	123.0(2)	123.4(1)	125.09(4)
N2−M1−O1	126.1(1)	126.2(1)	125.10(4)
O1−M1−O2	78.5(1)	80.95(9)	81.44(6)
M1−O1−M2	101.7(1)	99.05(9)	98.56(6)

[a] Data taken from refs 5 and 8. [b] This work.

The magnesium compounds **1** and **3** show variable-temperature NMR behavior consistent with the generalized equilibrium reaction shown in eq **1**,

$$LMgX\cdot THF \rightleftarrows LMgX + THF \qquad (1)$$

where X = O^{t}Bu and N^{i}Pr$_2$. The spectral behavior is similar in both CD_2Cl_2 and toluene-d_8, although compound **1** reacts with CD_2Cl_2. The VT ^{1}H NMR spectra obtained for **3** in toluene-d_8 are shown in Figure 7. By −10 °C, the equilibrium is slow on the NMR time scale and lies to the left, in favor of the THF adduct. Under similar conditions of concentration, the amide complex **1** does not show static THF complexation

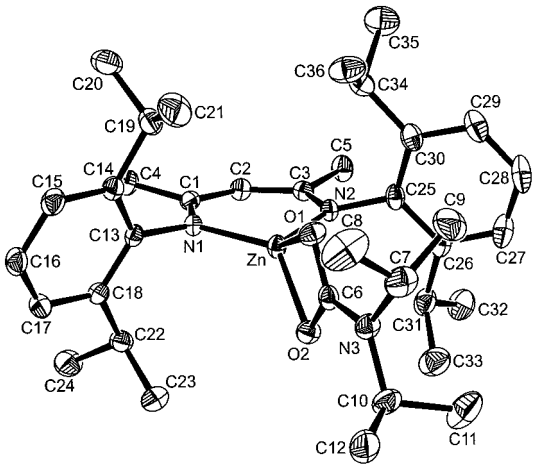

Figure 6. ORTEP drawing of LZn(η^2-$O_2CN^iPr_2$) with thermal ellipsoids drawn at the 50% probability level. Hydrogen atoms are omitted for clarity.

Table 7. Selected Bond Distances (Å) and Angles (deg) for LZn(η^2-$O_2CN^iPr_2$)

A	B	distance	A	B	C	angle
Zn	N1	1.935(1)	N1	Zn	N2	100.47(5)
Zn	N2	1.952(1)	N1	Zn	O1	127.57(4)
Zn	O1	2.028(2)	N2	Zn	O1	114.76(4)
Zn	O2	2.041(1)	N1	Zn	O2	129.43(4)
N3	C6	1.349(2)	N2	Zn	O2	117.69(4)

until ca. −70 °C. At −80 °C, we observe restricted rotation about the Mg−O THF bond. From this, we know that the equilibria are similar for both complexes but that THF complexation is more favored for the *tert*-butoxide compound **3**. This is understandable on the basis of both steric and electronic grounds.

In the presence of added THF, one can observe the exchange between free and coordinated THF such that, at room temperature, only one set of THF signals is seen, but at low temperatures, one sees signals for free and coordinated THF. See the Supporting Information. Most significantly, the coalescence temperature for the ^{i}Pr signals is not affected by the added THF. Indeed, even when spectra are recorded in neat THF-d_8, the coalescence behavior is remarkably similar, as shown in Figure 8 for the diisopropylamide complex **1**. The spectrum recorded at −60 °C in THF-d_8 corresponds to that expected for the complexed molecule. This indicates that, even in neat THF, the exchange mechanism is a dissociative interchange one based on the equilibrium **1**. Inspection of Figures 1 and 2 might have led one to anticipate a bimolecular THF exchange mechanism wherein as one Mg···O(THF) bond breaks, another forms at the opposite site. If an associative interchange mechanism were operative, this would generate a plane of symmetry as shown in **I** below. This would give rise to an NMR spectrum equivalent to that of a three-coordinate LMgX compound.

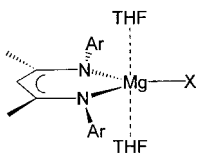

I

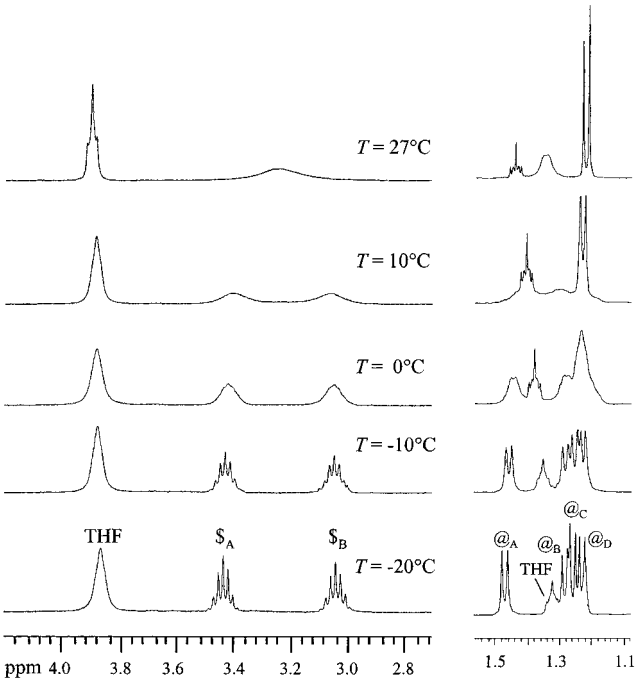

Figure 7. VT ^{1}H NMR spectra (toluene-d_8, 400 MHz) of LMg(O^{t}Bu)(THF), **3**, where $A and $B are C*H*MeMe′ and C*H*′Me′Me‴ protons, and @A, @B, @C, and @D are nonequivalent CH*Me*Me′, CH′*Me*′Me‴, CH′Me″*Me*‴, and CHMe*Me*′ protons.

In contrast to the coordination of THF to Mg^{2+} in compounds **1** and **3**, the LZn(OSiPh$_3$)·(THF) complex readily dissociates its THF in solution and exchange is rapid on the ^{1}H NMR time scale, even at −80 °C in toluene-d_8. The isolation of the Zn^{2+} 3-coordinate complex **2**, which is prepared in THF, clearly indicates that the equilibrium reaction that is related to **1** must lie to the right for zinc in related pairs of compounds.

NMR data for the above and other compounds described in this work are given in the Experimental Section.

Reactivity Studies. Ring-Opening Polymerizations of Lactides. All the compounds reported here will initiate and then sustain ring-opening polymerization of lactides (*L*-, *rac*- and *meso*-). The zinc (2+) compounds ultimately generate Coates' catalyst system[8] as previously described from reactions employing [LZn(μ-O^{i}Pr)]$_2$. From this work, we can obtain a clear dependence of the rate of initiation, which follows the order Mg > Zn and O^{t}Bu > N^{i}Pr$_2$ > NSi$_2$Me$_6$ > OSiPh$_3$. We feel that this order reflects both electronic and steric factors, so while N^{i}Pr$_2$ is clearly the most basic ligand, its lone pair is sterically less accessible than that of O^{t}Bu.

The relative order of the reactivities of the metals Mg > Zn was seen in a competition experiment wherein 1 equiv of lactide was allowed to react with an equimolar solution of LMNSi$_2$Me$_6$. Here, close to 100% (within NMR detection limits) of the LMgNSi$_2$Me$_6$ reacted, while the zinc analogue remained.

Coates and co-workers previously noted that [LZn(μ-O^{i}Pr)]$_2$ reacted with *meso*-LA to give syndiotactic PLA[5] (*sss* tetrads) and with *rac*-lactide to give heterotactic PLA[8] (∼90% *isi* + *sis* tetrads). It is therefore not surprising that we observe

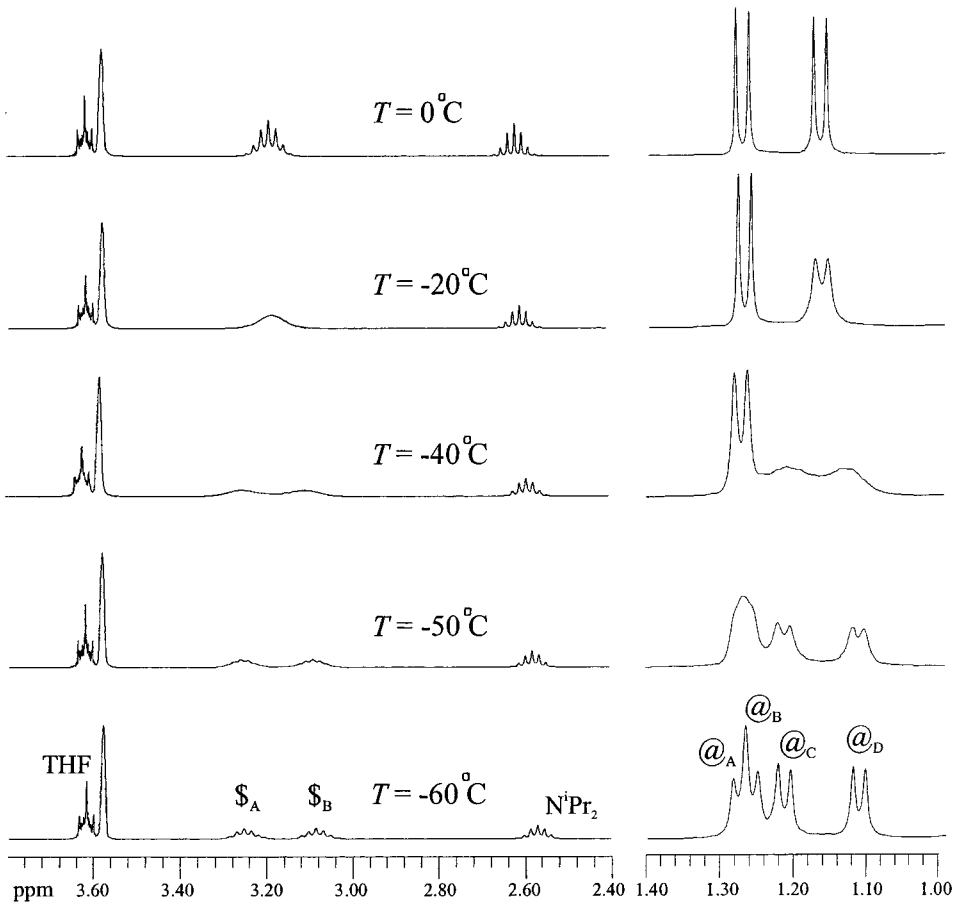

Figure 8. VT ^{1}H NMR spectra (THF-d_8, 400 MHz) of LMg(N^{i}Pr$_2$)(THF), **1**, where $\$_A$ and $\$_B$ are C*H*MeMe′ and C*H*′Me″Me‴ protons, and $@_A$, $@_B$, $@_C$ and $@_D$ are nonequivalent CH*Me*Me′, CH′*Me*″Me‴, CH′Me″*Me*‴, and CHMe*Me*′ protons.

that all the zinc compounds will react with *rac*-LA in CH_2Cl_2 to give similar stereoselectivity. However, the magnesium compounds **1** and **3** do not show this stereoselectivity in CH_2Cl_2 or benzene. (Compound **1** reacts with methylene chloride, presumably to abstract Cl and form LMgCl, and no polymerization of LA is observed.) The reaction between **3** and 100 equiv of LA is very rapid at room temperature in CH_2Cl_2, giving ca. 98% conversion within 2 min. The related zinc tertiary butoxide compound **4** gives ca. 95% conversion in 10 min under otherwise identical conditions. The initially formed PLA in reactions employing **1** and **3** and *rac*-LA conforms to a Bernoulian distribution of tetrads 3*iii*:2*isi*:*sis*:*iis*:*sii*.[11] With time, the magnesium catalyst system shows the formation of the other tetrads (*sss*, *ssi*, and *iss*) arising from transesterification. However, it is clear that the rate of ROP of LA is faster than the rate of transesterification.

We have also carried out the polymerization in THF solutions with rather interesting observations. First, the rates of polymerization are slower, but still rapid by most catalyst standards.[12] The related magnesium and zinc *tert*-butoxides, **2** and **4**, polymerized 100 equiv of *rac*-lactide to >95% conversion in 5 and 80 min, respectively. The somewhat slower rate of ROP is understandable in terms of competition for LA coordination to the metal center in the presence of the donor solvent, THF. Most interestingly, we observed that the magnesium catalyst system showed stereoselectivity in THF similar to that found for zinc. See Figure 9. The relative stereoselectivity shown by the zinc catalyst system was, however, not changed in THF relative to CH_2Cl_2.

A summary of the ring-opening polymerization of *rac*-lactide by the various magnesium and zinc compounds reported in this study is given in Table 8. The time to ca. 95% conversion is clearly seen to be dependent on the metal, the solvent, and the initiating group bound to the metal (this becomes the end-group of the growing polymer chain). With a slow initiation rate, relative to propagation, we observed large PDI values and higher molecular weight polymer as judged by the M_n values.

NMR Studies Aimed at Probing the Resting State of the Metal Centers. We allowed samples of the related magnesium and zinc *tert*-butoxide complexes **3** and **4** to react with L-LA (ca. 5 equiv.) in toluene-d_8 and THF-d_8 and then monitored the ^{1}H NMR spectrum as a function of temperature. As we have shown from studies of the binding of THF to the magnesium center in **3**, a four-coordinate metal center having $N_2MO(O')$ coordination, where O = an alkoxide and O′ = an O-donor such as THF or a ketonic group, will lead to the appearance of four isopropyl doublets. This is indeed seen for the zinc complex, as is shown in Figure 10. This is

(11) Kricheldorf, H. R.; Boettcher, C.; Tonnes, K. U. *Polymer* **1992**, *33*, 2817−2824.
(12) O'Keefe, B. J.; Hillmyer, M. A.; Tolman, W. B. *J. Chem. Soc., Dalton Trans.* **2001**, *15*, 2215−2224.

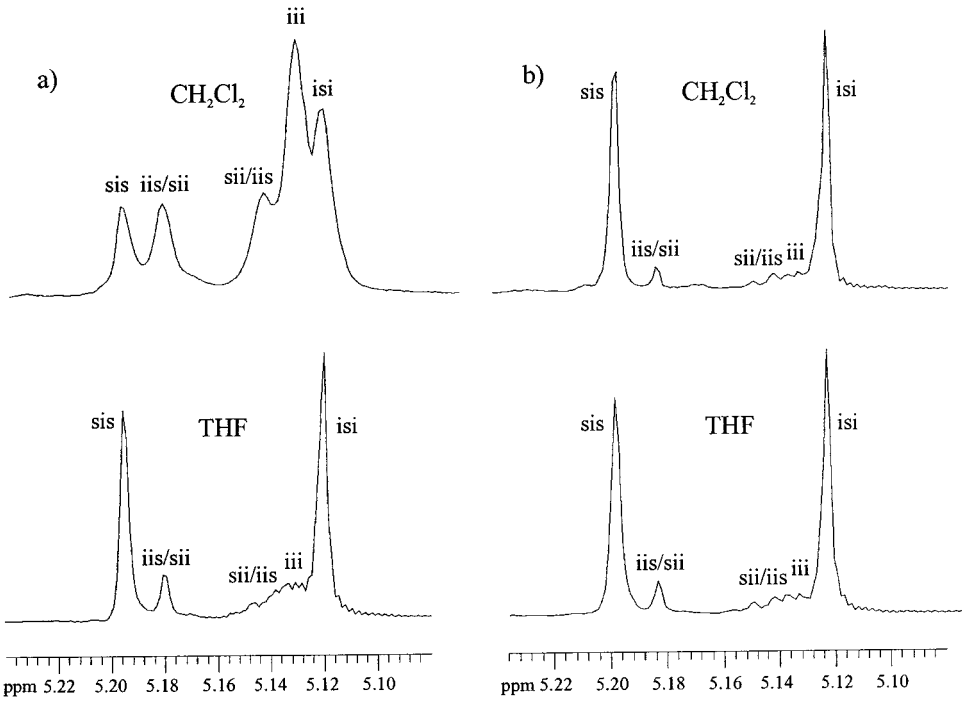

Figure 9. ^{1}H NMR spectra ($CDCl_3$, 400 MHz, 27 °C) of the homodecoupled C*H* resonance of poly(*rac*-lactide) prepared in CH_2Cl_2 and THF using (a) LMg(O^{t}Bu)(THF) and (b) LZn(O^{t}Bu) as initiators.

Table 8. Polymerization of *rac*-LA (100:1 [LA]:[catalyst]) in CH_2Cl_2 and THF at 20 °C Using the Magnesium and Zinc Complexes

entry	catalyst	solvent	time	convn (%)	$M_n \times 10^3$ (Da)	M_w/M_n
1	LMg(O^{t}Bu)·(THF)	CH_2Cl_2	2 min	97	19.8	1.49
2	LMg(O^{t}Bu)·(THF)	THF	5 min	95	14.6	1.47
3	LMg(N^{i}Pr$_2$)·(THF)	THF	5 min	94	13.3	1.60
4	LZn(O^{t}Bu)	CH_2Cl_2	10 min	95	16.0	1.15
5	LZn(O^{t}Bu)	THF	50 min	93	17.4	1.22
6	LZn(N^{i}Pr$_2$)	CH_2Cl_2	40 min	94	18.5	1.45
7	LZn(N^{i}Pr$_2$)	THF	100 min	93	19.6	1.37
8	LZnN(SiMe$_3$)$_2$	CH_2Cl_2	3 h	97	18.4	1.55
9	LZn(OSiPh$_3$)·(THF)	CH_2Cl_2	70 h	91	22.8	1.45

consistent with the view that the growing polymer chain binds to the metal center, as was seen, for example, in the model compound LZn(OCHMeC(O)OMe).[5] The resting state of LZn(OP) is illustrated in **II**.

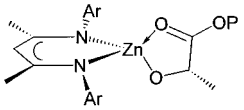

II

In contrast, the magnesium system shows only two isopropyl doublets for the β-diiminate ligand, even at −80 °C. See Figure 10. Given that we have established that magnesium binds THF more aggressively than zinc in the related alkoxide and amide complexes, the appearance of only two isopropyl doublets is at first surprising. We propose that this arises because the magnesium compound exists in solution as a dimeric molecule wherein the two magnesium atoms are united by a pair of alkoxide ligands from the growing polymer chain. This effectively creates a mirror plane of symmetry, as seen in the molecular structure of **7**.

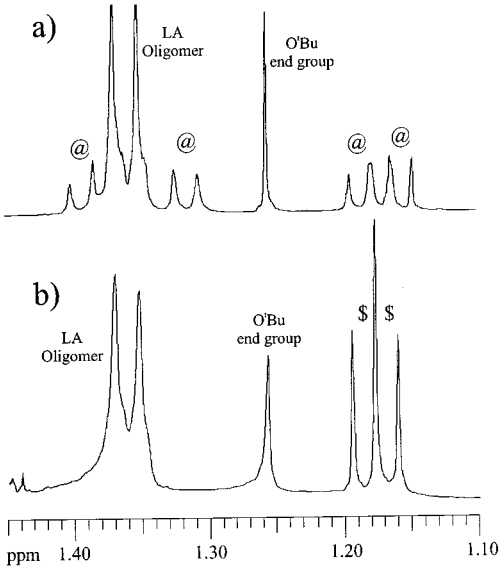

Figure 10. ^{1}H NMR spectra (toluene-d_8, 400 MHz, 27 °C) of isopropyl protons from the β-diiminate ligands when 5 equiv of L-LA was reacted with (a) LZnO^{t}Bu showing @ as four isopropyl doublets and (b) LMg(O^{t}Bu)(THF) showing $ as two isopropyl doublets.

The proposed resting state of LMg(OP) is depicted in **III**.

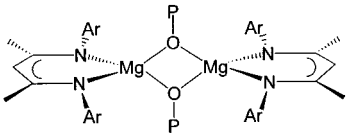

III

This, of course, does not mean that the active form of the magnesium catalyst system is not monomeric in THF, and this could account for the different stereoselectivity of polymerizations in THF versus toluene and methylene chloride.

Reactions with Propylene Oxide (PO) and Cyclohexene Oxide (CHO). The zinc compounds **2** and **4** in benzene showed no reactivity toward PO and CHO (1 and 5 equiv). Nor was there any reaction in the neat epoxide as solvent. Clearly these monomeric zinc compounds are not effective as homopolymerization catalyst precursors.

In contrast, the magnesium compounds **1** and **3** react in benzene with PO and CHO at room temperature. No isolable product has been obtained from the reactions involving PO, although we can state that PPO is not formed. In the case of CHO, compound **7** is formed in near quantitative yield and is obtained as colorless crystals from benzene. As shown by the crystallographic study, this compound results from ring-opening of CHO by allylic proton abstraction. Collectively, these findings further underscore the fact that ring-opening of epoxides by alkoxide ligands does not operate by a cis-migratory mechanism.[13] In this work, we see that the more basic alkoxide and amide ligands bound to magnesium may effect allylic proton abstraction. The inability to achieve homopolymerization of PO or CHO presumably arises because a bimolecular mechanism involving a reaction between an epoxide coordinated to one metal and an alkoxide ligand bound to another is not favorable.

Reactions with Carbon Dioxide. The magnesium compounds **1** and **3** react rapidly with CO_2 in hydrocarbon solutions, even at low temperatures. The materials produced are hydrocarbon-soluble but yield extremely complex ^{1}H NMR spectra. It seems that more than one compound is being formed and that we are quite probably getting insertion of CO_2 into a β-diiminato nitrogen bond as well as the N^iPr_2 or O^tBu group.

The reaction between CO_2 and hydrocarbon solutions of compound **2** react cleanly to form the carbamate $LZn(\eta^2\text{-}O_2CN^iPr_2)$, **8**, as the single detectable and isolable product. This insertion appears irreversible. Compound **8** does not react with either PO or CHO.

The reaction between CO_2 and compound **4** appears more complex, and no simple compound such as $LZnO_2CO^tBu$ has been isolated. However, compound **4** does react with PO and CO_2 to give propylene carbonate and with CHO and CO_2 to give the alternating copolymer of CHO−CO_2. In this regard, $LZnO^tBu$ shows similar reactivity to the Coates' catalyst $[LZn(\mu\text{-}O^iPr)]_2$, which is believed to act as a single-site catalyst.

Concluding Remarks

In the present study, we have prepared and characterized closely related monomeric magnesium and zinc alkoxide and amide complexes. This has allowed a detailed comparison of the coordination properties and reactivities of pairs of magnesium and zinc compounds. Magnesium shows a higher binding affinity toward donor ligands and a higher reactivity for its M−N and M−O bonds. The latter we can reasonably attribute to the greater polarity of M−X bonds for M = Mg relative to M = Zn, where X = OR or NR_2. Polymerization of lactide is notably faster for magnesium than for zinc, and *rac*-LA shows a remarkable solvent dependence in giving atactic PLA in CH_2Cl_2 versus heterotactic PLA in THF. Our ^{1}H NMR studies suggest that the resting state of the zinc complex during polymerization of lactide is a monomeric four-coordinate center, where the growing chain chelates to the metal center akin to that in $LZn(\eta^2\text{-}OCHMeC(O)OMe)$.[5] For magnesium, the major species present in solution is consistent with a dimer $LMg(\mu\text{-}OP)_2MgL$. These results underscore the intricacies of the fundamental steps in the reactions of LA and CHO/CO_2 recently reported by Coates and co-workers.[5,6] It is, for example, fascinating to note that $LZnO^tBu$ reacts with PO and CO_2 and CHO and CO_2 to give, respectively, propylene carbonate and the alternating co-polymer of CO_2 and CHO, whereas the compound $LZnN^iPr_2$ reacts with CO_2 in the presence of either PO or CHO to give only $LZn(\eta^2\text{-}O_2CN^iPr_2)$.

Experimental Section

General Considerations. The manipulation of air-sensitive compounds involved the use of anhydrous solvents and dry and oxygen-free nitrogen employing standard Schlenk line and drybox techniques. *rac*-Lactide was purchased from Aldrich and was sublimed three times prior to use. Tetrahydrofuran, dichloromethane, hexane, and toluene were distilled under nitrogen from sodium/benzophenone, calcium hydride, potassium metal, and sodium metal, respectively. The β-diiminato ligand $CH(CMeNC_6H_3\text{-}2,6\text{-}^iPr_2)_2$,[14] $LZnN(SiMe_3)_2$,[6] $LMgN(SiMe_3)_2$,[5] and $Mg(N^iPr_2)_2$[15] were prepared according to literature procedures. $LMg(O^tBu)(THF)$ may be synthesized according to our previous procedure,[7] but we prefer the one-pot synthesis described below. Hydrous $ZnCl_2$ was dried using chlorotrimethylsilane.[16] LiN^iPr_2 was prepared from the reaction of BuLi and HN^iPr_2. CO_2 gas was purchased from The BOC Group, Inc. and used as received. Anhydrous ^{t}BuOH was purchased from Aldrich and used as received. Cyclohexene oxide (CHO) and propylene oxide (PO) were distilled from calcium hydride under vacuum.

Measurements. ^{1}H and $^{13}C\{^1H\}$ spectra were recorded in C_6D_6, THF-d_8, CD_2Cl_2, and toluene-d_8 on Bruker DPX-400 NMR spectrometers and were referenced to the residual protio impurity peak (C_6D_6, δ 7.15; THF-d_8, δ 3.58; CD_2Cl_2, δ 5.32; toluene-d_8,

(13) Antelmann, B.; Chisholm, M. H.; Huffman, J. C.; Iyer, S. S.; Navarro-Llobet, D.; Pagel, M.; Simonsick, W. J.; Zhong, W. *Macromolecules* **2001**, *34*, 3159−3175.

(14) Feldman, J.; McLain, S. J.; Parthasarathy, A.; Marshall, W. J.; Calabrese, J. C.; Arthur, S. D. *Organometallics* **1997**, *16*, 1514−1516.

(15) Ashby, E. C.; Lin, J. J.; Goel, A. B. *J. Org. Chem.* **1978**, *43*, 1564−1566.

(16) Boudjouk, P.; So, J. H.; Ackermann, M. N.; Hawley, S. E.; Turk, B. E. *Inorg. Synth.* **1992**, *29*, 108−111.

2.09, for ^{1}H; and C_6D_6, δ 128.0; THF-d_8, δ 67.57; CD_2Cl_2, δ 53.8; toluene-d_8, 20.4, for $^{13}C\{^1H\}$). Elemental analyses were done by Atlantic Microlab, Inc. Gel permeation chromatography measurements were carried out using a Waters 1525 binary HPLC pump and Waters 410 differential refractometer equipped with styragel HR 2&4 columns (100 and 10 000 Å). The GPC was eluted with THF at 35 °C running at 1 mL/min and was calibrated using polystyrene standard. Mass spectrometry was done by electron impact ionization at 60 eV using a Kratos MS890 double-focusing magnetic-sector instrument at 6000 V ion-acceleration energy in the extended mass-range mode of the magnet.

LMg(N^{i}Pr$_2$)(THF), 1. THF (15 mL) was added to a mixture of LH (0.400 g, 0.956 mmol) and Mg(N^{i}Pr$_2$)$_2$ (0.215 g, 0.957 mmol). The solution was then refluxed for 3 h and cooled to room temperature. The volatile components were removed under a dynamic vacuum pump, giving a light green solid. Fine crystals were obtained by recrystallization in THF (0.36 g, 61%). MS (EI): m/z = 541.4 (M − THF)$^+$. ^{1}H NMR (C_6D_6): 7.16−7.20 (m, 6H, ArH), 4.77 (s, 1H, β-CH), 3.85 (m, 4H, O(C*H*$_2$CH$_2$)$_2$), 3.25 (sept, 4H, J = 6.9 Hz, C*H*Me$_2$), 2.96 (sept, 2H, J = 6.3 Hz, NC*H*Me$_2$), 1.64 (s, 6H, α-Me), 1.40 (m, 4H, O(CH$_2$C*H*$_2$)$_2$), 1.37 (d, 12H, J = 6.9 Hz, CH*Me*$_2$), 1.21 (d, 12H, J = 6.9 Hz, CH*Me*$_2$), 0.87 (d, 12H, J = 6.3 Hz, NCH*Me*$_2$). $^{13}C\{^1H\}$ NMR (C_6D_6): 168.46 (C═N), 147.07 (ipso-Ar), 142.30 (*o*-Ar), 125.34 (*p*-Ar), 124.02 (*m*-Ar), 94.82 (β-C), 70.09 (O*C*H$_2$), 47.79 (N*C*HMe$_2$), 28.45 (NCH*Me*$_2$), 28.34 (*C*HMe$_2$), 25.40 (O(CH$_2$*C*H$_2$)$_2$), 24.93 (CH*Me*$_2$), 24.87 (α-Me), 24.58 (CH*Me*$_2$).

LZn(N^{i}Pr$_2$), 2. THF (15 mL) was added to a mixture of LH (0.500 g, 1.2 mmol) and LiN^{i}Pr$_2$ (0.260 g, 2.43 mmol). The mixture was stirred for 30 min and then added to a solution of $ZnCl_2$ (0.163 g, 1.2 mmol) in 10 mL of THF dropwise. The solution was then stirred for 1 h and the solvent was removed under dynamic vacuum. The product was extracted with 20 mL of hexane, giving a light green solid (0.53 g, 76%). X-ray-suitable single crystals were obtained by placing a concentrated hexane solution in a freezer. MS (EI): m/z = 581.4 (M$^+$). ^{1}H NMR (C_6D_6): 7.12 (m, 6H, ArH), 4.94 (s, 1H, β-CH), 3.24 (sept, 4H, J = 6.8 Hz, C*H*Me$_2$), 2.87 (sept, 2H, J = 6.4 Hz, NC*H*Me$_2$), 1.68 (s, 6H, α-Me), 1.38 (d, 12H, J = 6.8 Hz, CH*Me*$_2$), 1.14 (d, 12H, J = 6.8 Hz, CH*Me*$_2$), 0.80 (d, 12H, J = 6.4 Hz, NCH*Me*$_2$). $^{13}C\{^1H\}$ NMR (C_6D_6): 168.94 (C═N), 145.54 (ipso-Ar), 141.94 (*o*-Ar), 126.13 (*p*-Ar), 124.21 (*m*-Ar), 94.98 (β-C), 48.81 (N*C*HMe$_2$), 28.74 (*C*HMe$_2$), 27.60 (NCH*Me*$_2$), 24.32 (CH*Me*$_2$), 24.25 (α-Me), 24.21 (CH*Me*$_2$).

LMg(OBu^t)(THF), 3. THF (15 mL) was added to a mixture of LH (0.400 g, 0.956 mmol) and Mg(N^{i}Pr$_2$)$_2$ (0.215 g, 0.957 mmol). The solution was then refluxed for 3 h and cooled to room temperature. To this solution was added ^{t}BuOH (95 μL, 0.99 mmol) via a microsyringe and the mixture stirred for 10 min. The volatile components were subsequently removed under dynamic vacuum, giving a white power (0.52 g, 93%). X-ray-suitable crystals were obtained by placing a concentrated THF solution in a freezer. MS (EI): m/z = 514.4 (M − THF)$^+$. ^{1}H NMR (CD_2Cl_2, −30 °C): 7.15 (m, 6H, ArH), 4.78 (s, 1H, β-CH), 4.02 (br, 4H, O(C*H*$_2$CH$_2$)$_2$), 3.16 (sept, 2H, J = 7.1 Hz, C*H*MeMe′), 2.95 (sept, 2H, J = 7.1 Hz, C*H*′Me″Me‴), 1.96 (br, 4H, O(CH$_2$C*H*$_2$)$_2$), 1.60 (s, 6H, α-Me), 1.22 (d, 6H, J = 7.1 Hz, CH*Me*Me′), 1.19 (d, 6H, J = 7.2 Hz, CH′*Me*″Me‴), 1.13 (d, 6H, J = 6.7 Hz, CH′Me″*Me*‴), 1.05 (d, 6H, J = 6.7 Hz, CHMe*Me*′), 0.57 (s, 9H, O^{t}Bu).

LZnO^{t}Bu, 4. A solution of LZn(N^{i}Pr$_2$) (0.500 g, 0.858 mmol) in 15 mL of toluene was cooled to −78 °C. A precooled (−78 °C) solution of ^{t}BuOH (82 μL, 0.86 mmol) in 10 mL of toluene was then added dropwise to the zinc complex solution. The mixture was allowed to warm slowly to room temperature and stirred for 15 min. The volatile liquid was removed under dynamic vacuum, giving white solid (0.44 g, 92%). X-ray-suitable crystals were grown by placing a concentrated toluene solution in a freezer overnight. MS (EI): m/z = 554.3 (M$^+$). Anal. Calcd for $C_{33}H_{50}N_2OZn$: C, 70.29; H, 8.87; N, 4.97. Found: C, 70.31; H, 8.92; N, 5.08. ^{1}H NMR (C_6D_6): 7.11 (m, 6H, ArH), 4.91 (s, 1H, β-CH), 3.16 (sept, 4H, J = 6.9 Hz, C*H*Me$_2$), 1.66 (s, 6H, α-Me), 1.40 (d, 12H, J = 6.9 Hz, CH*Me*$_2$), 1.15 (d, 12H, J = 6.9 Hz, CH*Me*$_2$), 0.96 (s, 9H, O^{t}Bu). $^{13}C\{^1H\}$ NMR (C_6D_6): 169.48 (C═N), 143.89 (ipso-Ar), 141.77 (*o*-Ar), 126.29 (*p*-Ar), 123.89 (*m*-Ar), 94.87 (β-C), 68.66 (O*C*Me$_3$), 35.41 (OC*Me*$_3$), 28.62 (*C*HMe$_2$), 24.36 (CH*Me*$_2$), 23.71 (CH*Me*$_2$), 23.64 (α-Me).

(BDI)ZnOSiPh$_3$.(THF), 6. A solution of Ph_3SiOH (0.215 g, 0.778 mmol) in 10 mL of THF was added slowly to a solution of (BDI)ZnN(SiMe$_3$)$_2$ (0.500 g, 0.778 mmol) in 5 mL of THF. The resulting clear solution was stirred overnight and the solvent was removed, giving a white powder (0.613 g, 95%). ^{1}H NMR (CD_2Cl_2, δ): 7.30 (t, 2H, J = 7.8 Hz, *p*-^{i}Pr$_2$ArH), 7.18 (d, 4H, J = 7.8 Hz, *m*-^{i}Pr$_2$ArH), 7.13 (m, 3H, *p*-SiArH), 7.01 (t, 6H, J = 6.7 Hz, *m*-SiArH), 6.92 (m, 6H, *o*-SiArH), 5.09 (s, 1H, β-CH), 3.68 (m, 4H, O(C*H*$_2$CH$_2$)$_2$), 3.00 (heptet, 4H, J = 7.2 Hz, C*H*MeMe′), 1.82 (m, 4H, O(CH$_2$C*H*$_2$)$_2$), 1.79 (s, 6H, α-Me), 1.20 (d, 12H, J = 6.9 Hz, CH*Me*Me′), 0.90 (d, 12H, J = 6.9 Hz, CHMe*Me*′).

[LMg(μ-OC$_6$H$_9$)]$_2$, 7. Cyclohexene oxide (15 μL, 0.015 mmol) was added to a solution of LMgN(SiMe$_3$)$_2$ (0.049 g, 0.081 mmol) or LMg(N^{i}Pr$_2$)(THF) (0.050 g, 0.081 mmol) in 5 mL of benzene. The mixture was stirred for 15 s and then left without stirring overnight. X-ray-suitable colorless crystals were formed and separated by filtration (0.080 g, 95%). MS (EI): m/z = 1077.8 (M$^+$).

LZn(η^2-O$_2$CN^{i}Pr$_2$), 8. LZn(N^{i}Pr$_2$) (0.500 g, 0.858 mmol) was dissolved in 15 mL of benzene. CO_2 gas was bubbled through the solution for 10 min and solvent was removed under dynamic vacuum, giving a white solid in quantitative yield. X-ray-suitable crystals were obtained by placing the concentrated THF solution in a freezer. Anal. Calcd for $C_{36}H_{55}N_3O_2Zn$: C, 68.92; H, 8.85; N, 6.70. Found: C, 68.97; H, 8.76; N, 6.59. ^{1}H NMR (C_6D_6): 7.00−7.12 (m, 6H,ArH), 4.94 (s, 1H, β-CH), 3.55 (sept, 2H, J = 6.8 Hz, NC*H*Me$_2$), 3.37 (sept, 4H, J = 6.9 Hz, C*H*Me$_2$), 1.72 (s, 6H, α-Me), 1.48 (d, 12H, J = 6.9 Hz, CH*Me*$_2$), 1.18 (d, 12H, J = 6.9 Hz, CH*Me*$_2$), 0.83 (d, 12H, J = 6.8 Hz, NCH*Me*$_2$). $^{13}C\{^1H\}$ NMR (C_6D_6): 169.29 (C═N), 166.49 (O_2CN), 143.51 (ipso-Ar), 142.42 (*o*-Ar), 126.04 (*p*-Ar), 123.76 (*m*-Ar), 94.19 (β-C), 46.12 (N*C*HMe$_2$), 28.45 (*C*HMe$_2$), 24.32 (CH*Me*$_2$), 24.17 (CH*Me*$_2$), 23.50 (α-Me), 20.74 (NCH*Me*$_2$).

General Polymerization Procedure. *rac*-Lactide (0.500 g, 3.47 mmol) was dissolved in 6.0 mL of CH_2Cl_2 or THF. A solution of the corresponding catalyst (0.0347 mmol) in 1.5 mL of CH_2Cl_2 or THF was then added to the lactide solution (100:1 [lactide]:[catalyst]). The reaction was stirred at room temperature for the desired period, at which time small aliquots were taken to monitor the conversion. When the conversion is greater than 90%, the polymerization was quenched with excess methanol. The polymer precipitate was then filtered and dried under vacuum to constant weight.

General Epoxides/CO_2 Copolymerization Procedure. Epoxides (34.6 mmol) and the corresponding catalyst (0.0346 mmol) (1000:1 [epoxide]:[catalyst]) were placed in a 40-mL stainless steel

Table 9. Summary of Crystallographic Data

compound	**1**	**2**	**3**	**4**	**7**	**8**
empirical formula	$C_{39}H_{63}MgN_3O$	$C_{35}H_{55}N_3Zn$	$C_{37}H_{58}MgN_2O_2$	$C_{33}H_{50}N_2OZn$	$C_{70}H_{100}Mg_2N_4O_2 + C_6D_6$	$C_{36}H_{55}N_3O_2Zn$
formula weight	614.23	583.19	587.18	556.12	1162.31	627.20
color	pale yellow	colorless	colorless	colorless	colorless	colorless
crystal size (mm)	0.23 × 0.38 × 0.38	0.08 × 0.35 × 0.42	0.4 × 0.4 × 0.15	0.23 × 0.46 × 0.46	0.15 × 0.23 × 0.35	0.27 × 0.27 × 0.38
crystal system	orthorhombic	monoclinic	monoclinic	orthorhombic	monoclinic	monoclinic
space group	Pbca	$P2_1/m$	$P2_1$	$Pca2_1$	$C2/m$	$P2_1/n$
cell dimensions						
temp (K)	200	200	111	150	150	150
a (Å)	18.273(1)	8.911(1)	9.7999(3)	17.3061(2)	17.9210(2)	12.0085(1)
b (Å)	18.636(1)	20.807(2)	16.6069(5)	21.2069(3)	19.7085(3)	20.5887(1)
c (Å)	22.520(2)	10.058(1)	11.5815(3)	17.8377(2)	11.5343(2)	14.7710(1)
β (deg)		113.585(1)	109.345(1)		123.072(1)	104.378(1)
Z	8	2	2	8	2	4
volume (Å^3)	7669.05(9)	1709.13(3)	1778.43	6546.6(1)	3413.84(9)	3537.59(4)
d_{calc} (g/cm^3)	1.064	1.133	1.097	1.128	1.131	1.178
λ (Å)	0.71073	0.71073	0.71073	0.71073	0.71073	0.71073
abs coeff (cm^{-1})	0.078	0.744	0.082	0.775	0.083	0.727
θ range (deg)	2.12−25.01	2.42−27.46	0−30	2.25−27.50	2.06−27.47	2.20−27.49
reflns collect.	121866	29064	27281	88477	31417	62379
indpndnt reflns	6743	4013	8177	14581	4027	8113
R1(F)[a] [$I > 2\sigma(I)$]	0.0632	0.0355	$R(F)$[b] = 0.0327	0.0541	0.0509	0.0302
R1(F)[a] (all data)	0.0858	0.0454		0.112	0.0796	0.0400
wR2(F^2)[a] (all data)	0.195	0.0924		0.148	0.141	0.0809
goodness of fit	1.024	1.042	0.633	1.010	1.047	1.049

[a] $R1(F) = \sum||F_o| - |F_c||/\sum|F_o|$; $wR2(F^2) = \{\sum w(F_o^2 - F_c^2)^2/\sum w(F_o^2)^2\}^{1/2}$; $W = 1/[\sigma^2(F_o^2) + (xP)^2 + yP]$; $P = (F_o^2 + 2F_c^2)/3$, where $x = 0.1005$, $y = 4.5413$ for **1**; $x = 0.0434$, $y = 0.6374$ for **2**; $x = 0.0570$, $y = 6.3321$ for **4**; $x = 0.0680$, $y = 1.8580$ for **7**; $x = 0.0416$, $y = 0.9763$ for **8**. [b] $R(F) = \sum||F_o| - |F_c||/\sum|F_o|$; $R_w(F) = \{\sum w(|F_o| - |F_c|)^2/\sum w|F_o|^2\}^{1/2}$, where $w = 1/[|\sigma^2||F_o|]$.

reactor equipped with a stirring bar. CO_2 (100 psi) was then charged to the reactor. The reaction was stirred at the desired temperature and time. After CO_2 gas was released, a small aliquot was taken to determine the conversion. The polymerization was then quenched with excess methanol. The polymer was subsequently filtered and dried under vacuum to constant weight.

X-ray Crystallography. Single-crystal X-ray diffraction data were collected on a Nonius Kappa CCD diffractometer at low temperature using an Oxford Cryosystems Cryostream Cooler (Table 9). Crystals were coated with oil prior to being placed in the nitrogen gas stream. The data collection strategy was set up to measure a quadrant of reciprocal space for compounds **7** and **8**, an octant for **1** and **4**, a hemisphere for **2** and **5**, with a redundancy factor of 1.9, 2.7, or 4, which means that 90% of the reflections were measured at least 1.9, 2.7, or 4 times, respectively. A combination of ψ and ω scans with a frame width of 1.0° was used. Data integration was done with Denzo.[17] Scaling and merging of the data was done with Scalepack.[17] The structures were solved by either the Patterson method or direct methods in SHELXS-86.[18] Full-matrix least-squares refinements based on F^2 were performed in SHELXL-93.[19] The methyl group hydrogen atoms were added at calculated positions using a riding model with $U(H) = 1.5U_{eq}$(bonded C atom). For each methyl group, the torsion angle that defines its orientation about the C−C bond was refined. The other hydrogen atoms were included in the model at calculated positions using a riding model with $U(H) = 1.2U_{eq}$(bonded C atom). Neutral atom scattering factors were used and include terms for anomalous dispersion.[20]

Acknowledgment. We thank the Department of Energy, Office of Basic Sciences, Chemistry Division for financial support of this work. K.P. acknowledges the Institute for the Promotion of Teaching Science and Technology (IPST), Thailand, for an opportunity to work on this project.

Supporting Information Available: Crystallographic data for compounds **1**−**5**, **7**, and **8**; VT ^{1}H NMR spectra of LMg(O^{t}Bu)(THF). This material is available free of charge via the Internet at http://pubs.acs.org.

IC020148E

(17) Otwinowski, Z.; Minor, W. *Methods in Enzymology, Vol. 276: Macromolecular Crystallography*, Carter, C. W., Jr., Sweet, R. M., Eds.; Academic Press: New York, 1997; Part A, pp 307−326.

(18) Sheldrick, G. M. *Acta Crystallogr.* **1990**, *A46*, 467−473.

(19) Sheldrick, G. M. Universitat Gottingen, Germany, 1993.

(20) *International Tables for Crystallography;* Kluwer Academic Publishers: Dordrecht, 1992; Volume C.